Microstructuring of Polymer Films by Inkjet Etching

I. A. Grimaldi,[1,2] A. De Girolamo Del Mauro,[1] G. Nenna,[1] F. Loffredo,[1] C. Minarini,[1] F. Villani[1]

[1]*Italian National Agency for New Technologies, Energy and Sustainable Economic Development (ENEA), Portici Research Center, Piazzale Enrico Fermi 1, 80055 Portici (Naples), Italy*
[2]*Department of Physics, University of Naples "Federico II," Via Cintia 1, 80126 Naples, Italy*

Received 28 April 2011; accepted 28 April 2011
DOI 10.1002/app.34776
Published online 11 August 2011 in Wiley Online Library (wileyonlinelibrary.com).

ABSTRACT: The inkjet printing (IJP) technique is generally used as tool for positioning small quantities of a liquid material on a target substrate. An interesting application of IJP is inkjet etching that consists of the deposition of drops of solvent or solvent mixtures onto a soluble polymer layer. This technique allows one to structure the polymer film and to change the shape, from concave to convex, by varying the mixing ratio of the solvents. In this work, the structuring of some polymeric layers (polyimide and polystyrene) by solvents [*N*-methyl-2-pyrrolidone (NMP) and toluene (TOL)] and a solvent mixture (TOL–NMP) at different mixing ratios were studied, and the effect of the printing parameters on the microstructural profile was investigated. Some applications in optoelectronic devices are described. © 2011 Wiley Periodicals, Inc. J Appl Polym Sci 122: 3637–3643, 2011

Key words: microstructure; morphology; thin films

INTRODUCTION

The structuring of materials is employed for different applications, such as the generation of biochips and micropatterned cell arrays,[1,2] patterning for building bank structures,[3] the fabrication of microlens arrays,[4,5] and the texturing of surfaces[6] to improve the efficiency of organic light-emitting diode (OLED) and photovoltaic devices.[7,8] Several methods have been proposed for polymer microstructuring, and normally, they use multiple process steps. Recently, inkjet etching (IJE), an application of inkjet printing (IJP) technology, was proposed as an alternative single-process technique. IJP, a tool for precisely positioning small volumes of liquid material onto a substrate, is emerging for its capability of patterning and large-area processing, efficient use of material, reduced waste products, and low cost of process. In particular, IJE consists of the deposition of a pure solvent or a mixture of solvents onto a soluble polymer layer to create microstructures whose shape is a function of the mixing ratio.

In general, when a single solvent drop is printed, a crater-shaped microstructure is created on the top of the polymer surface. Indeed, when the solvent drop hits the polymer layer, the polymer is locally dissolved, carried from the sessile drop center to the edges and deposited there. This phenomenon occurs because of the maximum evaporation rate and the drop pinning at the three-phase contact line.[9–13] The motion of this convective flow inside the drop and directed toward its rim leads to an ununiform solute deposition with an accumulation of material at the edges at the end of the drying process.[14,15] This phenomenon is known as the *coffee-stain effect*.[9,12,16,17] Additionally, the redistribution of the polymer dissolved by a single solvent drop also depends on the contribution of Marangoni flow but in less significant way than the convective flow. Marangoni flow is related to the temperature gradient of the sessile drop and, hence, to the different surface tensions at the droplet liquid–air interface and generates a solute motion from droplet rim to the center.[18] The contribution of Marangoni flow becomes more important in the definition of the final profile of the polymer when a dual-solvent system formed by solvents with different evaporation rates is employed. When a mixture of high- and low-boiling point solvents is used, a concentration gradient of one solvent opposite to the concentration gradient of the other solvent is generated along the sessile drop radius. In this case, the solvent volatility and the surface tension properties combined with the mixing ratio allow one to control the capillary flows inside the droplet and to vary the microstructural shape from concave to convex.

Moreover, by changing the number of the drops of pure solvent or solvent mixture, the morphological properties and the geometry of the structures also change.[13]

Correspondence to: I. A. Grimaldi (angelica.grimaldi@enea.it).
Contract grant sponsor: Technology and Research for the Application of Polymer in Electronic Devices (TRIPODE) project, financed by the Ministero dell'Università e della Ricerca; contract grant number: DM 20160.

In this work, microstructures were fabricated on polyimide (PI) and polystyrene (PS) layers by IJP of *N*-methyl-2-pyrrolidone (NMP) and toluene (TOL) drops, respectively. The PS layer was also structured by a TOL–NMP mixture with different mixing ratios. The effects of the printing parameters on the microstructural profile were investigated through profilometric and optical microscopy analyses. Some applications of the manufactured structuring were realized.

EXPERIMENTAL

Commercial glass substrates purchased from Schott were cleaned by sonication with deionized water, acetone and isopropyl alcohol, dried with nitrogen, and finally placed in oven at 130°C for 1 h.

After the cleaning process, the PI and PS polymeric films were deposited on glass substrates by means of a Brewer Science model 100 spin coater (Rolla, MO). The PI film, 1 μm thick, was spun at 5000 rpm for 30 s with a 2-mL volume of a commercial solution (PI 2556) purchased from HD Microsystems. The PS sample was deposited with 2 mL of a solution of commercial PS (Aldrich, weight-average molecular weight ≈ 350,000) dissolved in chlorobenzene at 90°C for 30 min with a concentration of 15% (w/w). The PS film thickness was 5.3 μm and was spin-coated at 500 rpm for 20 s.

All of the polymeric samples were placed on a hot plate at 100°C for 15 min to completely remove the solvent.

Successively, drops of NMP and TOL were inkjet-printed onto the PI and PS layers, respectively. Moreover, the structuring of the PS film was also performed by the printing of TOL–NMP mixtures at different mixing ratios (1 : 1, 1.5 : 1, 1.8 : 1, 2 : 1, 2.3 : 1, and 3 : 1). NMP was chosen for the PI structuring because the precursor monomers of the purchased PI were dissolved in it. As for the PS structuring, the choice of TOL as the single-solvent system and TOL and NMP as mixture components arose from the fact that both dissolve the PS layer and are miscible together. Furthermore, these solvents have different volatility and surface tension properties (TOL: $T_b = 110.6$°C, $\gamma = 28.53$ mN/m; NMP: $T_b = 202$°C, $\gamma = 40$ mN/m; where T_b is the boiling temperature and γ is the surface tension), and their evaporation rates are suitable for IJP processing.

The droplet depositions were performed by means of inkjet equipment especially designed by Aurel S.p.A (Modigliana, Italy). for the printing of inks on flexible substrates as a reel or single sheet and not flexible substrates. This printer uses the piezoelectric drop-on-demand technology to eject droplets through a microdrop printhead (50- or 70-μm opening nozzle with a 90- or 180-pL droplet volume, respectively). Moreover, the system allows one to control the substrate temperature from the ambient conditions [ambient temperature (T_{amb})] to 50°C. As for the PS layer, sequences of TOL and TOL–NMP droplets were printed by means of the 50-μm opening nozzle printhead at a 6.7-Hz drop emission frequency and a 1 mm/s printhead speed with a spacing between the droplets of 160 μm; this created a square array of microstructures on the polymer layer. Similarly, for the PI layer, sequences of NMP droplets were printed by means of the 70-μm opening nozzle printhead at a 5-Hz drop emission frequency and a 2 mm/s printhead speed with a spacing between the droplets of 400 μm.

After the structuring, only PI samples were thermally treated with a curing process at 200°C for 30 min in air and at 300°C for 1 h in a nitrogen atmosphere.

A surface profilometer (KLA Tencor P-10 surface profiler) and an optical microscope (Polyvar MET Reichert-Jung, Depew, NY) were used to detect and analyze the morphology and the profile of each manufactured microstructure.

RESULTS AND DISCUSSION

PI structured by NMP

Through IJP of NMP drops onto the PI polymer film, crater-shaped microstructures formed on the polymer surface at the end of the solvent evaporation. The typical two-dimensional profile of the microstructure had a central spherically shaped cavity and two lateral humps, as shown in Figure 1. In Figure 1, the structural parameters that characterized the microcrater profile are also reported: W_c is the width at the cavity bottom ($W_c = 0$ in the case represented in Fig. 1), W_0 is the internal diameter, W_e is the diameter at the cavity top, W_{tot} is the external diameter, H_{ec} is the total depth of the cavity, and finally, H_e and H_c are the edge height and the cavity depth, respectively, with reference to the unstructured external polymer surface. These geometrical parameters were used to quantitatively monitor the microstructural profile changes by variation of the printing conditions. The profilometric analysis employed to determine the profile and its structural parameters was also used to investigate the root-mean-square roughness inside the cavity, which was about 10–15 nm. Moreover, this investigation showed that there were no cracks on the microstructured polymer surface; this indicated, combined with the roughness information, the structured polymer could be used in good quality optical applications.

Furthermore, the profile reported in Figure 1 also shows that the depth of the microcavity realized by the printing of the single drop was, by far, less than the thickness of the PI film (1 μm).

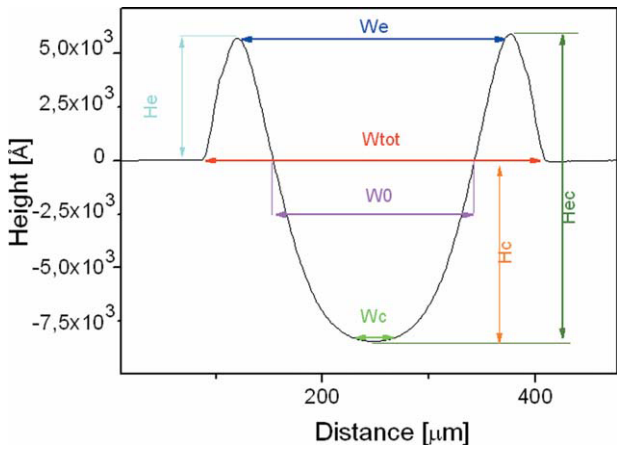

Figure 1 Profile of the microcavity manufactured by the printing of an NMP drop on PI film and its geometrical parameters. [Color figure can be viewed in the online issue, which is available at wileyonlinelibrary.com.]

To investigate the effect of the number of the printed drops (N_D) on the microstructural geometry, single and multiple drops were deposited onto the polymer layer. The profiles of the manufactured microstructure by the printing of one, two, and three NMP drops onto the PI film are reported in Figure 2(a). As the number of the inkjet-printed droplets increased, the microcavity geometrical parameters also increased. Figure 2(b,c) shows the values of the microstructural parameters as a function of N_D. It can be observed that the external diameter increased less significantly than the total depth as N_D increased. This can be explained as follows. With the exception of the first inkjet-printed droplet, which hit a uniform polymer surface, the next droplets, deposited with the same volume and in the same place as the first one after a certain delay, met the cavity-shaped polymer surface and converged toward its bottom. Thus, the multiple droplets removed the polymer mainly from the cavity bottom rather than from its edges; this appreciably modified the total depth (47% variation) and left the external diameter almost invariable (9% variation).

The flat bottom of the microcavity manufactured by IJP of three NMP drops indicated that the volume amount of the deposited solvent was enough to dissolve and completely remove the polymer along all of the thickness to reach the undersubstrate.

The effect of the substrate temperature on the microstructural profile was also investigated. In Figure 3 is reported the profile of the PI microstructure fabricated by the printing of a single NMP droplet onto the polymer layer and with the substrate kept at 50°C for comparison with the microstructure manufactured at T_{amb}. Moreover, the profiles of the samples manufactured in the same temperature conditions and with two NMP droplets deposited were also characterized, and the geometrical parameter values are shown in Figure 4. The results of Figures 3 and 4 indicate that the higher temperature induced a cavity diameter decrease and a depth increase because of the fact that it made the polymer softer, and in addition, the deposited droplet, evaporating

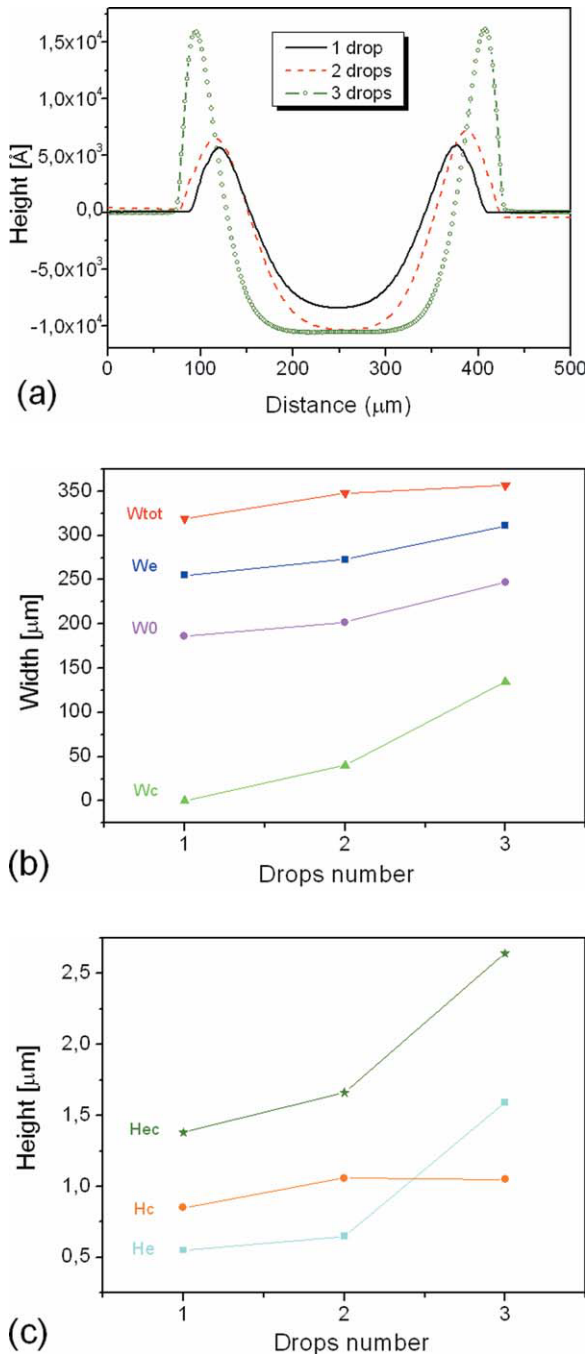

Figure 2 (a) Profiles of the PI microstructures manufactured by the printing of one, two, and three drops of NMP. Geometrical parameters of each cavity, (b) diameter and (c) depth, as function of the number of drops. [Color figure can be viewed in the online issue, which is available at wileyonlinelibrary.com.]

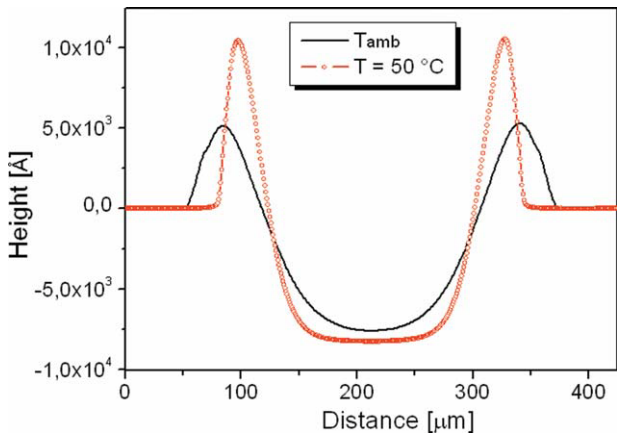

Figure 3 Profiles of the PI microstructures manufactured by the printing of an NMP single drop with the substrate at T_{amb} and heated at $T = 50°C$. [Color figure can be viewed in the online issue, which is available at wileyonlinelibrary.com.]

more quickly, wet a smaller polymer surface. It is important to highlight that the temperature (T) of 50°C was lower than the requested one for inducing the PI curing process. The effect of multiple drops on the geometrical parameters at higher temperature was the same as that observed at T_{amb}. Furthermore, the polymer film temperature appeared as the printing parameter that influenced the microstructural profile in a more significant manner.

After structuring, the PI film was thermally cured, turning completely insoluble to NMP solvent. Indeed, the cure heating cycle (at 200°C for 30 min in air and at 300°C for 1 h in a nitrogen atmosphere) converted the precursor film [poly(amic acid)] to insoluble PI and dried out the remaining solvent. The heat treatment of the precursor film caused a drastic change in the backbone structures toward stiffer and more planar chain structures and induced dramatic changes in the mechanical properties. In confirmation, tests of the printing of NMP drops onto the treated polymer film demonstrated that no polymer surface structuring could be performed, and so no microstructure could be further created.

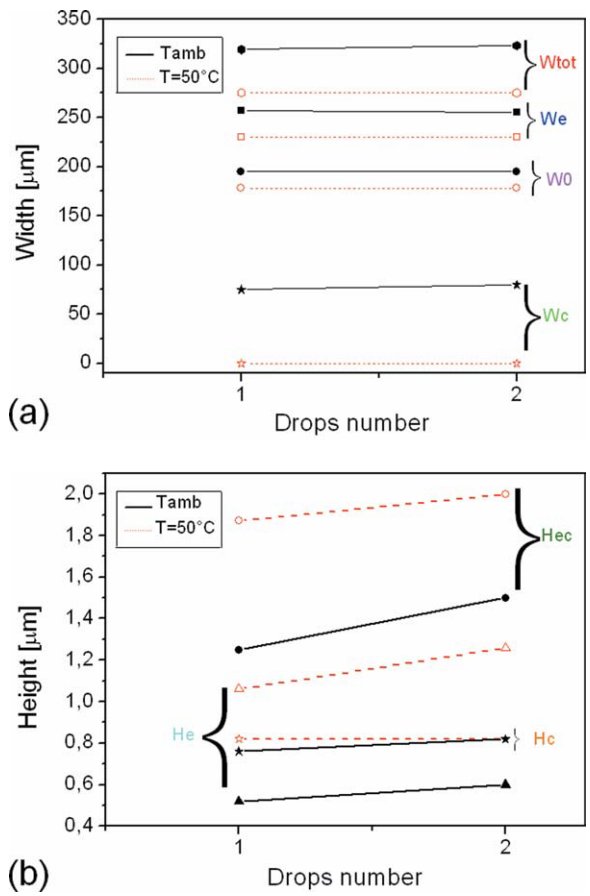

Figure 4 Geometrical parameters, (a) diameter and (b) depth, of the cavities fabricated at T_{amb} and $T = 50°C$ as a function of the number of the printed NMP drops. [Color figure can be viewed in the online issue, which is available at wileyonlinelibrary.com.]

PS structured by TOL

Preliminary printing tests were performed with several solvents (TOL, NMP, *n*-butyl acetate, tetrahydrofuran, benzene) on the PS polymer film to define the process parameters that were useful for creating repeatable structures. For whatever solvent, it was observed that the 50°C substrate temperature was the necessary condition for the repeatability of the microstructuring process. Because the solvent droplet deposited on the heated polymer layer evaporated more rapidly, the drying process and the polymer redistribution were so fast that fewer variables were involved in the structuring process; this allowed better control of the microstructural profiles. Therefore, all of the prints on the PS layer, described

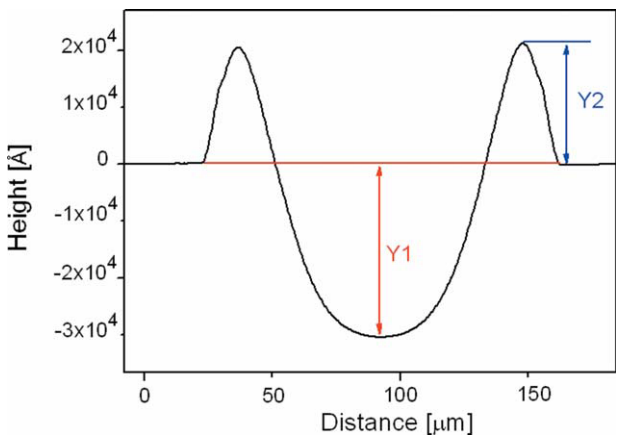

Figure 5 Profile of the microcavity manufactured by the printing of a TOL drop on the PS film and its geometrical parameters. [Color figure can be viewed in the online issue, which is available at wileyonlinelibrary.com.]

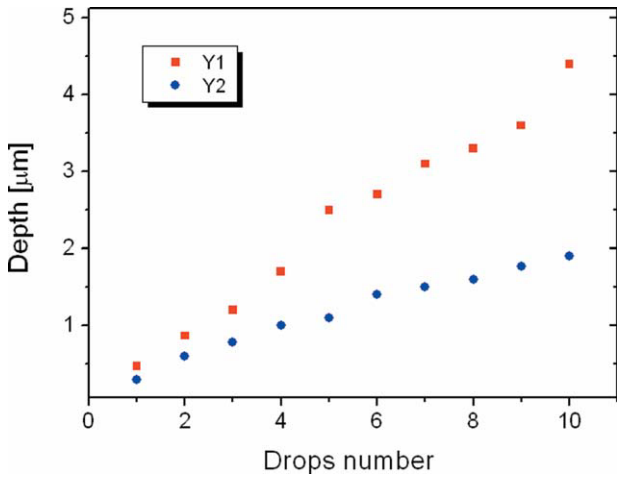

Figure 6 PS microcavity geometrical parameters (Y_1 and Y_2) as a function of the number of TOL drops. [Color figure can be viewed in the online issue, which is available at wileyonlinelibrary.com.]

in the following, were carried out with the heated substrate (50°C).

The microstructural profile obtained by the printing of a single TOL drop on the PS layer, shown in Figure 5, was crater-shaped and was very similar to the one performed on the PI film structured by NMP. The influence of N_D on the microcavity geometrical parameters was analyzed for this solvent–polymer system, too. As in the study of PI structured by NMP it was demonstrated that the effect of the multiple droplets was more dominant on the cavity depth rather than on the diameter; the same behavior was observed with the TOL–PS system. With regard to the depth parameters, namely, the cavity depth and the edge height with reference to the unstructured external polymer surface (Y_1 and Y_2 in Fig. 5, respectively), they linearly increased as function of N_D, as shown in Figure 6.

PS structured by TOL–NMP

Successively, PS structuring was carried out by the use of a dual-solvent system. The profiles of the manufactured structures on the PS layer by the deposition of single drops of mixtures of TOL and NMP at different volume ratios and with the heated substrate (50°C) are shown in Figure 7. The copresence of different solvents in the droplet induced a polymer redistribution after its dissolution that basically depended on the chemicophysical properties of each solvent and also on the volume ratio in the mixture. In detail, after the mixture drop deposition, the fast evaporation at the sessile drop rim left there a higher concentration of the less volatile component (NMP) that in this case, had the higher surface tension and promoted a Marangoni flow from the center to the edge. When the more volatile component (TOL) content was increased, most of the dissolved polymer piled up in the center, as is clear in Figure 7 for the TOL–NMP mixing ratios ranging from 1.8 : 1 to 2.3 : 1. A further increase in the TOL content in the mixture (TOL–NMP 3 : 1) modified the microstructure and generated a complex shape with a crater on the pile top. This was the consequence of the created compositional gradient, which generated an additional flow from the outer edge to the center, which was already visible in the profile related to the 1 : 1 mixing ratio, shown in Figure 7. Indeed, the rim of this profile was characterized by two humps on the same side and was more evident when compared to the profile of the microstructure realized by the pure solvent drop (Fig. 5); the internal one, in particular, was just due to the flow directed toward the inside.

The study of the effect of the number of the deposited mixture drops on the structural profile confirmed that already observed for the single-solvent systems. For each fixed mixing ratio, a higher number of droplets modified the profile geometrical parameters; precisely, the depth and height increased more significantly than the diameter and left the shape almost unaltered.

Applications

The concave- and convex-shaped microstructures were manufactured and characterized for different applications, mainly those focused on the improvement of OLED device efficiency.

In particular, the structured PI layer was employed as a template for another polymer that models itself and acquires a complementary shape. The employed polymer solution was commercial Sylgard 184 silicone elastomer (Dow Corning,

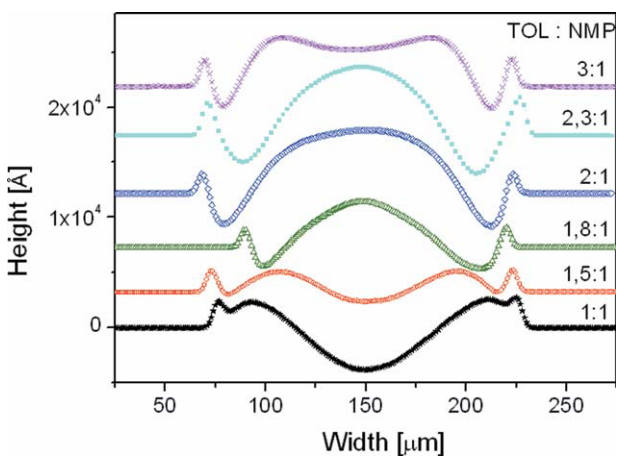

Figure 7 PS microstructural profiles realized by the printing of TOL and NMP mixture drops at different mixing ratios. [Color figure can be viewed in the online issue, which is available at wileyonlinelibrary.com.]

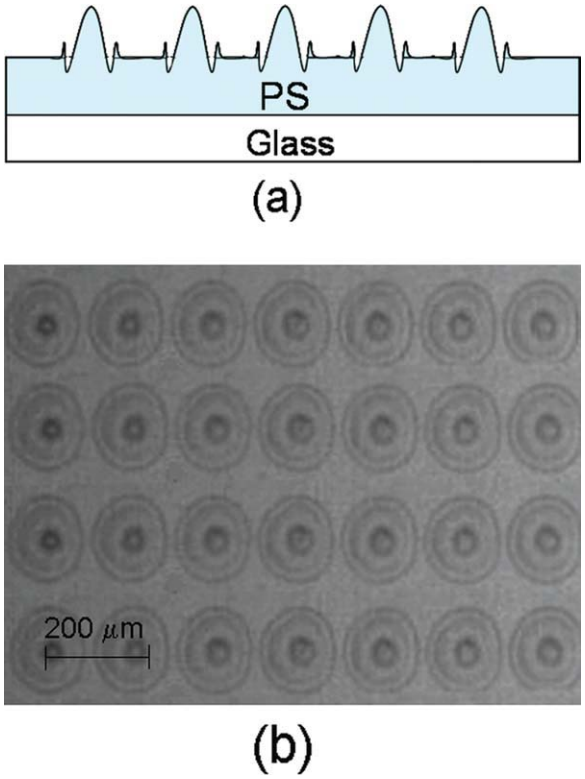

Figure 8 (a) Schematic section and (b) optical micrograph of a PS microlens array. [Color figure can be viewed in the online issue, which is available at wileyonlinelibrary.com.]

Midland, MI) mixed with a curing agent at a mixing ratio of 10 : 1; after being placed into a vacuum chamber to remove the bubbles, it was spin-coated on the microstructured PI layer at 5000 rpm for 60 s, leaving a thickness of about 1 μm. Successively, after a curing process at 100°C for 45 min, the elastomeric silicone polymer was removed from the PI mold; this resulted in a convex-shaped structuring on top of its surface, that is, the complementary form with respect to the profile in Figure 1.

This convex-shaped microstructuring, as well as the convex-shaped structuring manufactured with the TOL–NMP–PS system, can be used as microlenses. For this purpose in particular, a square array of microlenses was fabricated with a 5×5 mm^2 surface by the deposition of multiple drops of the TOL–NMP mixture with a mixing ratio of 2.3 : 1 on the PS layer. In Figure 8, the schematic section and the optical micrograph of the PS microlens array are illustrated.

A preliminary study was performed on the employment of these polymer microstructures in OLED devices for improving the outcoupling efficiency. The PS polymer with suitable optical properties and the microstructural geometry could reduce the electroluminescent (EL) radiation losses due to the total internal reflection. Therefore, the manufactured microlens array was coupled to an EL device, and a preliminary analysis of the electrooptical properties of the structured devices indicated emission efficiency increases of about 4% compared to an unstructured OLED.

The PS structuring with the profile shown in Figure 5 could be employed for texturing of the substrate of an OLED device. Through the printing of TOL multiple drops on the PS film, a square array of microcavities was fabricated, and the related schematic section and optical micrograph are reported in Figure 9. A detailed study was developed that demonstrated that this kind of structuring performed on a polymeric underlayer of a bottom-emitting OLED device allowed us to destroy the interference effects that were visible in the device emission spectrum.[19]

CONCLUSIONS

The feasibility of using the IJE technique to perform polymer microstructures was investigated. The microstructural profile could be controlled by the use of suitable solvents. It was demonstrated that the microstructural shape could be varied from concave to convex with a pure solvent or solvent mixtures with suitable mixing ratios. The geometrical parameters of the structures could also be modified by changes in the substrate temperature and/or N_D. Finally, some applications of these polymer microstructures to OLED devices were described, which demonstrated that they could better guide the generated EL radiation externally.

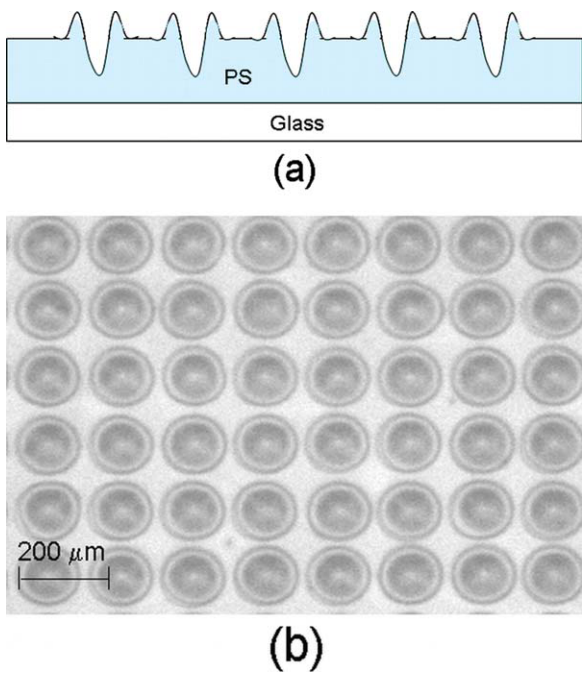

Figure 9 (a) Schematic section and (b) optical micrograph of a PS microcavity array. [Color figure can be viewed in the online issue, which is available at wileyonlinelibrary.com.]

References

1. Bouaidat, S.; Berendsen, C.; Thomsen, P.; Guldager Petersen, S.; Wolff, A.; Jonsmann, J. Lab Chip 2004, 4, 632.
2. Hyun, J.; Ma, H.; Zhang, Z.; Beebe, T. P.; Chilkoti, A. Adv Mater 2003, 15, 576.
3. Xia, Y.; Friend, R. H. Appl Phys Lett 2007, 90, 253513.
4. Chang, C. Y.; Yang, S. Y.; Sheh, J. L.; Microsyst Technol 2006, 12, 754.
5. Pericet-Camara, R.; Best, A.; Nett, S. K.; Gutmann, J. S.; Bonaccurso, E. Opt Exp 2007, 15, 9877.
6. Kapur, R.; Spargo, B. J.; Chen, M.; Calvert, J. M.; Rudolph, A. S. J Biomed Mater Res 1996, 33, 205.
7. Huang, W.-K.; Wang, W.-S.; Kan, H.-C.; Chen, F.-C. Jpn J Appl Phys 2006, 45, L1100.
8. Lennon, A. J.; Ho-Baillie, A. W. Y.; Wenham, S. R. Solar Energy Mater Solar Cells 2009, 93, 1865.
9. Deegan, R. D.; Bakajin, O.; Dupont, T. F.; Huber, G.; Nagel, S. R.; Witten, T. A. Nature 1997, 389, 827.
10. Deegan, R. D. Phys Rev E 2000, 61, 475.
11. Deegan, R. D.; Bakajin, O.; Dupont, T. F.; Huber, G.; Nagel, S. R.; Witten, T. A. Phys Rev E 2000, 62, 756.
12. de Gans, B.-J.; Hoeppener, S.; Schubert, U. S. Adv Mater 2006, 18, 910.
13. de Gans, B.-J.; Hoeppener, S.; Schubert, U. S. J Mater Chem 2007, 17, 3045.
14. Kawase, T.; Sirringhaus, H.; Friend, R. H.; Shimoda, T. Adv Mater 2001, 13, 1601.
15. Bonaccurso, E.; Butt, H. J.; Hankeln, B.; Niesenhaus, B.; Graf, K. Appl Phys Lett 2005, 86, 124101.
16. Tekin, E.; Holder, E.; Kozodaev, D.; Schubert, U. S. Adv Funct Mater 2007, 17, 277.
17. Ikegawa, M.; Azuma, H. JSME Int J B 2004, 47, 490.
18. Hu, H.; Larson, R. G. J Phys Chem B 2006, 110, 7090.
19. Villani, F.; Grimaldi, I. A.; Nenna, G.; De Girolamo Del Mauro, A.; Loffredo, F.; Minarini, C. Opt Lett 2010, 35, 3333.